*Egypt. J. Chem.* **Vol. 66**, No. 10 pp. 269 - 281 (2023)

**Egyptian Journal of Chemistry**

**http://ejchem.journals.ekb.eg/**

# Fabrication of Modified Chitosan with Furanone Derivatives and its Nanocomposites: Synthesis, Characterization and Evaluation as Anticancer Agents

**Mai Ali[a], Nadia G. Kandile[b], Mansoura I. Mohamed[b], Azza T. Taher[c,d], Hemat M. Mohamed[b,*]**

[a]*Department of Chemistry, Faculty of Pharmacy, October 6 University (O6U), October 6 City, Giza 12585, Egypt*

[b]*Chemistry Department, Faculty of Women for Art, Science and Education,Ain Shams University, Heliopolis Post Cod. No. 11757, Cairo, Egypt*

[c]*Department of Pharmaceutical Organic Chemistry, Faculty of Pharmacy, Cairo University, Cairo 11562, Egypt*

[d]*Department of Pharmaceutical Organic Chemistry, Faculty of Pharmacy, October 6 University (O6U), October 6 City, Giza 12585, Egypt*

**Abstract**

Cancer isone of the global health problems and the most frightening and fatal disease of human. With the rapid development of nanotechnology, nanocomposite**s** were used to improve antitumor therapeutic efficiency. Chitosan CS possesses many biological functions including antitumor due to its nontoxicity, biocompatibility, and biodegradability. The aim of the present work is the modification of CS with furanone derivatives **3A** or**3B** to give CS-I and CS-II derivatives respectively using microwave-assistant as a green technique to enhance the antitumor properties of CS. Nanocomposites were prepared by assembling Au, Ag orZnO NPs on CS-I and CS-II derivatives. Structures of CS-I, CS-II derivatives, and its nanocomposites were confirmed using different spectroscopic tools. The antitumor efficiency was assayed against two kinds of cancer cells **HepG-2** hepatocellular cancer and **MCF-7** breast cancer. CS-I and CS-II derivatives revealed a significant decrease in cancer cells viability reached to 13.69±2.03% and 10.54±0.92% against **HepG-2** respectively and 16.85±2.13% and 11.39±0.97% against **MCF-7** respectively compared to 25.48±1.66% and 26.76±1.96% for CS respectively. Additionally, nanocomposites showed superior cell viability and CS-I ZnONPs and CS-I Ag NPs derivatives showed the lowest value reached to 4.84±0.51% and 5.41±0.63% against **HepG-2**and**MCF-7** respectively.It was indicated that the new modified CS derivatives and its nanocomposites could be served as potential anticancer agents.

*Keywords:* Chitosan, Furanone, Nanocomposites, Antitumor activity.

## 1. Introduction

Cancer is now one of the more feared diseases, and chemotherapy is considered as important strategy for lowering the cancer rate [**1**]. Cancer treatment requires bioavailable, effective, and safe therapeutic agents. Recent advances in complementary and alternative medicine are investigating chemopreventive natural products that inhibit carcinogenesis and have strong anti-carcinogenic properties [**2**]. Biocompatible polymer-derived metal nanoparticles are benefit greatly in chemotherapeutic drug delivery, nanomedicine, and detection of tumor cells.Mostly noble metal nanoparticles have always been favored over other metal nanoparticles because of their superiority optical properties, biocompatibility and low cytotoxicity [**3**]. Nanoparticles, especially inorganic metals as gold, silver, iron, zinc, magnesium, or copper can significantly enhance anticancer, antioxidant and antibacterial activities of chitosan [**3-7**].

Chitosan is one of the attractive linear polysaccharides that is obtained by deacetylation of chitin and is composed of (β-1,4)-N-glucosamine and (β-1,4)-N-acetyl glucosamine units [**7-19**]. Chitosan is used in pharmaceutical and biomedical applications in different shapes as films, gels, micro and nanoparticles [**20**]. Chitosan has antitumor, hypolipidemic, anti-inflammatory, antibacterial and other biological activities due to its unique properties

*Corresponding author email:hemat.hassan@women.asu.edu.eg, alnada_mostfa@yahoo.com

EJCHEM use only: Received: 08 January 2023; Revise: 18 January 2023; Accepted: 18 January 2023

DOI:10.21608/EJCHEM.2023.186011.7432

as biodegradability, biocompatibility and non-toxicity [**21-25**].

In addition to its physicochemical properties, surface modifications of CS play an important role in the cytotoxic profile and targeting of cancers with rapid division and aggressive growth [**26**].

The present study aimed to modifyCS with heterocyclic compounds 3-(5-(4-methoxyphenyl)-2-oxofuran-3(2H)-ylidene) indolin-2-one **3A** or new derivative5-fluoro-3-(5-(4-methoxyphenyl)-2-oxofuran-3(2H)-ylidene) indolin-2-one**3B** and characterized the new CS derivatives by FTIR, elemental analysis, SEM, TGA and XRD. The nanocomposites of the new CS derivatives were formulated by loading inorganic nanoparticles as Au, Ag, orZnO on new CS derivatives and characterized by TEM. Finally, evaluation of their cytotoxic activities toward two cancer cells **HepG-2** and **MCF-7**.

## 2. Materials and methods

### 2.1. Materials

Chitosan CS (degree of deacetylation (DD) 93.3%, low molecular weightMW 60 KDa) was obtained from (Acros, Belgium). Isatin (indoline-2,3-dione) or 5-fluoroisatin (5-fluoroindoline-2,3-dione), were provied from (Sigma-Aldrich, USA). Tetrachloroauric acid $HAuCl_4$ and ZnO NPs were provided from (Alfa Aesar, Germany). Glacial acetic acid, acetic anhydride, sodium acetate, and silver nitrate were purchased (Edwic, Egypt). Absolute ethanol and dimethylformamide DMF were purchased from (Merck, Germany) and (Caloarba, France) respectively. All aqueous solutions were prepared using deionized and distilled water.

### 2.2. Experimental

#### 2.2.1. General procedure for Synthesis of 3-(5-(4-methoxyphenyl)-2-oxofuran-3(2H)-ylidene) indolin-2-one 3A or 5-fluoro-3-(5-(4-methoxyphenyl)-2-oxofuran-3(2H)-ylidene) indolin-2-one 3B

Furanone derivatives **3A** [**27**] and **3B**were prepared according to our previous work [**27**], via condensation of β-(p-methoxybenzoyl) propionic acid (0.01 mol) and isatin**1A** or 5-fluoroisatin **1B** (0.01 mol) in acetic anhydride (10 ml) in presence of fused sodium acetate (0.01 mol) as catalyst. The reaction mixture was irradiated in a microwave oven for 2 min at (400 W, 50 Hz, 230 V). The reaction mixture was cooled, and the precipitate was filtered off, washed with water and petroleum ether (b.p. 40–60 $^oC$). The solid product was crystallized from acetic acid to give **3A**m.p 216-218$^oC$ and yield 70%.

##### 2.2.1.1. 5-Fluoro-3-(5-(4-methoxyphenyl)-2-oxofuran-3(2H)-ylidene) indolin-2- one 3B

Dark brown solid, yield 50 %; mp 230-232$^oC$; $^1H$ NMR: d 9.12 (s, 1H, NH), 8.59-7.07 (m, 7H, 2Ar-H), 6.80 (s, 1H, CH), 3.83 (s, 3H, $CH_3$ of $CH_3O$-Ar) ppm, $^{13}C$ NMR d: 195.89, 189.37, 158.24, 139.16, 138.16, 137.67, 136.15, 129.51, 122.10, 115.77, 101.96, 100.00, 62.84. Anal. $C_{19}H_{12}FNO_4$ (337): Calcd: C, 67.65; H, 3.56; N, 4.15; Found: C, 67.51; H, 3.68; N, 4.37. Ms: m/z 338 $M^{+1}$ (3.98%).

#### 2.2.2. Modification of CS with furanone derivatives 3A or 3B

A clear CS solution was prepared by dissolving (0.6 g) into glacial acetic acid (30 mL) under stirring at room temperature for 1h. Solutions of furanone derivatives **3A** or **3B** (0.3 g) in DMF (2mL) and fused sodium acetate anhydrous (0.06 g) were added to CS solution. The reactions mixtures were stirred for 2 h at room temperature followed by irradiation in microwave oven [**28,29**]for (5×2) min at (300 W, 50 Hz, 230 V). The gel formed after cooling at room temperature was washed with DMF to remove the unreacted furanone derivatives then aqueous NaOH to neutralize the excess of glacial acetic acid. Finally, the gel was washed with distilled water and left to dry in an oven at 60$^oC$ to give CS-I or CS-II derivatives in dark red color.

#### 2.2.3. Synthesis of gold nanoparticles Au NPs

Gold nanoparticles Au NPs was prepared by reduction method using trisodium citrate. Deionized water was used for preparation of $HAuCl_4$ solution (2 mL, 1% wt/v) which diluted to (200 mL) then heated under stirring to boiling temperature. To boiling solution, trisodium citrate solution (2.5 mL, 1% wt/v) was added dropwise until the solution color changed to purple referred to the formation of Au NPs which confirmed by UV measurements and TEM [**7,17**].

#### 2.2.4. Synthesis of silver nanoparticles Ag NPs

Trisodium citrate was used to reduced silver nitrate $AgNO_3$ to prepare the colloidal silver nanoparticles solution. Trisodium citrate (5 mL, 1% wt/v) was added drop by drop under stirring to boiling $AgNO_3$ solution (50 mL, $1\times10^{-3}$ M). The reaction mixture was vigorously stirred and boiled until a pale-yellow color was appeared pointed to the formation of Ag NPs which confirmed by UV measurements and TEM [**7,17**].

#### 2.2.5. Loading of Au, Ag and ZnO NPs on CS-I or CS-II

Chitosan derivatives CS-I or CS-II (0.1g) were soaked in acetic acid (5 mL, 1%v/v) for 3 h then Au or Ag NPs solution (10 mL) or ethanolic solution of

ZnO NPs (10 mL, 0.1% wt/v) was added drop by drop and left under stirring for 24 h at room temperature. The nanocomposites were collected using centrifuge at (8,000 rpm for 30 min) and dried in oven at 60°C [**7**].

### 2.3. Characterizations of CS, new CS derivatives, and its nanocomposites

#### 2.3.1. Determination of the average molecular weight of CS

The average molecular weight MW of CS was determined using viscometry method at 25°C (a Brookfield viscometer). A buffer solution of acetic acid (0.1 M) and sodium chloride (0.2 M) was used to prepare different concentrations of CS solution. The viscosity of buffer solution and CS solutions was measured three times and the relative viscosity (η) was calculated. Based on the intrinsic viscosity [η] Mark–Houwink–Sakurada's empirical equation (**Eq.** (**1**)) [**19**] was used to calculate chitosan (MW)

$$[\eta] = k M^{a} \quad (1)$$

Where $k = 1.81\times10^{-3}$ and $a = 0.93$ for the buffer solution at 25°C.

#### 2.3.2. Elemental Analysis

A Perkin-Elmer 2400 C, H, N elemental analyzer were performed to determine elemental analyses that based on the traditional Pregl-Dumas method, in which samples are burned in a pure oxygen environment and the resulting combustion gases are measured automatically. For detection (TCD), a thermal conductivity detector is used. Total C, H, and N are measured with (0.1 g) precision. Element ratios are more important because they reduce instrument error. Molar element ratios can be reported accurately to three decimal places.

#### 2.3.3. FTIR spectroscopy

Fourier Transform Infrared (FTIR) spectra were measured using a Thermo Scientific Smart Omni-Transmission instrument via casting a thin film onto a KBr plate. The FTIR spectrum was measured in the range 4000–400 $cm^{-1}$ wave number.

#### 2.3.4. Thermogravimetric Analysis (TGA)

Thermogravimetric analysis (TGA) was obtained using the SDT Q600 V20.9 Build 20, USA under an inert nitrogen atmosphere at a heating rate of 10 °C/min. The sample capacity was (350 mg) including sample holder and temperatures ranging from 25 °C to 800 °C.

#### 2.3.5. X-Ray Diffraction Analysis (XRD)

The crystalline and amorphous nature of the prepared CS derivatives was investigated using X-ray diffraction analytical X'PERT PRO. Cu K radiation as the X-ray source. The sample was thoroughly grounded and scanned at 2θ degree range from 1–50.

#### 2.3.6. Ultraviolet Visible Spectroscopy

Ultraviolet Visible measurements for the prepared solution of Au, Ag and ZnO NPs were carried out by UV–vis photometer UV-2800BMS Scientific Technical Corporation (PVT) Ltd.

#### 2.3.7. Morphological Studies

##### 2.3.7.1. Scanning Electron Microscopy (SEM)

The morphological characterization and imaging were studied using A Scanning Electron Microscope (SEM). The samples were coated with gold after being mounted on a metal stub with double stick adhesive tape. The thickness of the gold film was 150 A°. The samples were then examined using a Quanta 250 FEG (Field Emission Gun) and an EDX unit (Energy Dispersive X-ray Analysis).

##### 2.3.7.2. Transmission Electron Microscopy (TEM)

Transmission Electron Microscope (TEM) was used to determine the shape and size of the nanoparticles. The samples were sonicated for 15 minutes before being placed on a carbon-coated copper grid. The coated grids were measured using a JEM - 1200 EX 2, Electron Microscope Jaban Specimens for (TEM).

### 2.4. In vitro cytotoxicity study

#### 2.4.1. Cancer cell cultures

**HepG-2** hepatocellular cancer and **MCF-7** breast cancer mammalian cell lines were obtained from the VACSERA Tissue Culture Unit. The cells were grown in Dulbecco's modified Eagle's medium (DMEM), thatcontained foetal bovine serum(10% heat-inactivated), L-glutamine(1%), (HEPES buffer), and gentamycin(50 g/ml). All cells were kept at 37°Cin a hydrated conditions with $CO_2$ (5%) and were subcultured for 15 days.

#### 2.4.2. Viability Assay

The viability assay was used to evaluate the cytotoxicity of CS, new CS derivatives and its nanocomposites. The cells were seeded in a 96-well plate, at a cell concentration of ($1\times10^{4}$) cells per well in (100 µL) of growth medium. Fresh medium containing the tested samples with different concentrations was added after 24 h of seeding. Serial two-fold dilutions of the tested samples were added to confluent cell monolayers using a multichannel pipette and dispensed into 96-well. The microtiter plates were incubated for 24 h at 37°C in a hydrated incubator with $CO_2$ (5%). Three wells were used for each concentration of the test polymer. With or without the tested samples, control cells were incubated, and additionally with or without DMSO (maximum 0.1%). The colorimetric method was used

to determine the viable yield using with crystal violet solution (1%) added to each well for at least 1/2 h. To remove any remaining stain, the plates were rinsed with tap water. To all wells, glacial acetic acid (30%) was added, and the absorbance of the plates was measured on a microplate reader (TECAN, Inc.) at a wavelength of 490 nm. Background absorbance detected in wells without added stain was corrected in all results [**30,31**].

**2.5. Statistical Analysis.**

Each of the tests were presented as the average value with its standard deviation (mean ± S.D) of each sample that is repeated three times (n=3). When the p-value was less than 0.05A, the difference was considered statistically significant.

## 3. Results and discussion

### 3.1. *Chemistry*

**3.1.1. Synthesis of 3-(5-(4-methoxyphenyl)-2-oxofuran-3(2H)-ylidene) indolin-2-one 3A or 5-fluoro-3-(5-(4-methoxyphenyl)-2-oxofuran-3(2H)-ylidene)indolin-2-one 3B**

Isatin (1H-indole-2,3-dione) and its derivatives showed a broad spectrum of biological activities such as antifungal, antibacterial, anti-inflammatory, antiviral, anticancer and anti-convulsant drug [**32**].

In this study, furanone derivatives **3A** [**27**]and **3B** were prepared by Perkin condensation reaction of isatin or 5-fluoroisatin **1A** or **1B** and β-(p-methoxybenzoyl) propionic acid (2) under microwave irradiation that reported in our previous study [**27**] (**Scheme 1**).The structure of new furanone derivative **3B** was confirmed by elemental analysis, $^{1}$HNMR, $^{13}$CNMR and mass spectrum (experimental part). Additionally, **Fig. 1A** represented FTIR spectrum for furanone derivative **3B** that showed characteristic absorption stretching vibration bands at 3119 $cm^{-1}$ for (NH), 3074, 2934 and 2840 $cm^{-1}$ displayed CH aromatic and aliphatic stretching vibration respectively. Three peaks at 1783 and 1717 $cm^{-1}$ referred to (C=O lactone) and 1698 $cm^{-1}$ ascribed to (C=O amide).

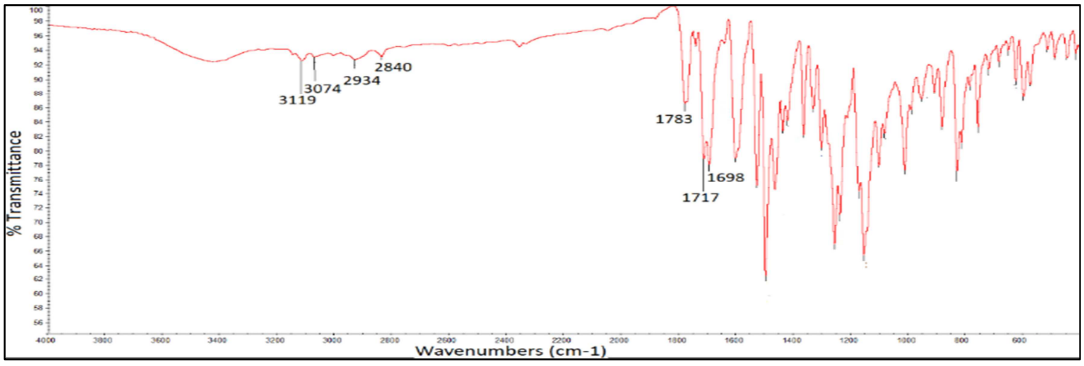


**Fig. 1A**: FTIR of 5-fluoro-3-(5-(4-methoxyphenyl)-2-oxofuran-3(2H)-ylidene) indolin-2-one **3B**

**3.1.2. Preparation of CS derivatives CS-I and CS-II**

It has been reported that simple chemical modifications to biocompatible polymers can improve physical and medical properties. As a natural polysaccharide, chitosan can be easily modified with other compounds due to the large number of reactive hydroxyl and amine groups on its backbone [**3**].

Two new CS derivatives CS-I and CS-II were prepared from the reaction of CS with furanone derivatives **3A**or**3B**using microwave-assisted method [**28,29**] (**Scheme1**). The structures of CS derivatives CS-I and CS-II were characterized by FTIR, elemental analysis, TGA, XRD, and SEM.

### 3.2. Characterization of CS, CS derivatives CS-I and CS-II and its nanocomposites

**3.2.1. Viscometry and Elemental Analysis**

The average molecular weight (MW) of (CS) was determined using the viscometry method of Mark-Houwink-Sakurada [**19**] and it approximately 60 KDa as shown in (**Table 1**).

The degree of deacetylation (the percentage of free amine group) for CS was calculated from **(Eq. (2)** [**33**] using elemental analysis of CS and the percentage employed in this study was 93.3%. The percentage of carbon, hydrogen, nitrogen, and degree of deacetylation of (CS) were represented in (**Table 1**).

$$DD\% = 1 - \left[ \frac{(C/N) - 5.145}{6.861 - 5.145} \right] \times 100 \qquad (2)$$

Where C/ N ratio displayed C% and N% for CS, and 5.145 and 6.861 values referred to N-deacetylated chitosan ($C_6H_{11}O_4N$) and N-acetylated chitin ($C_8H1_3O_5N$) repeat unit, respectively.

Table 1 also showed the degree of substitution (DS) for CS derivatives CS-I and CS-II was (0.13 and 0.15) respectively which was calculated using the following [**Eq. (3)**][**15**] and based on the ratio between C% and N% for CS and its derivatives. Low degree of substitution (DS) may be attributed to the difficult modification with the bulky furanone derivatives **3A** or**3B** and few number of ($NH_2$) group were involved in the reaction with furanone derivatives [**7,8,10**].

$$DS = \left[ \frac{(C/N)_m - (C/N)_i}{n} \right] \qquad (3)$$

Where $(C/N)_m$ and $(C/N)_i$ referred to C/N ratios for CS derivatives and CS respectively and (n) was the number of carbon atoms introduced into CS backbone after the modification.

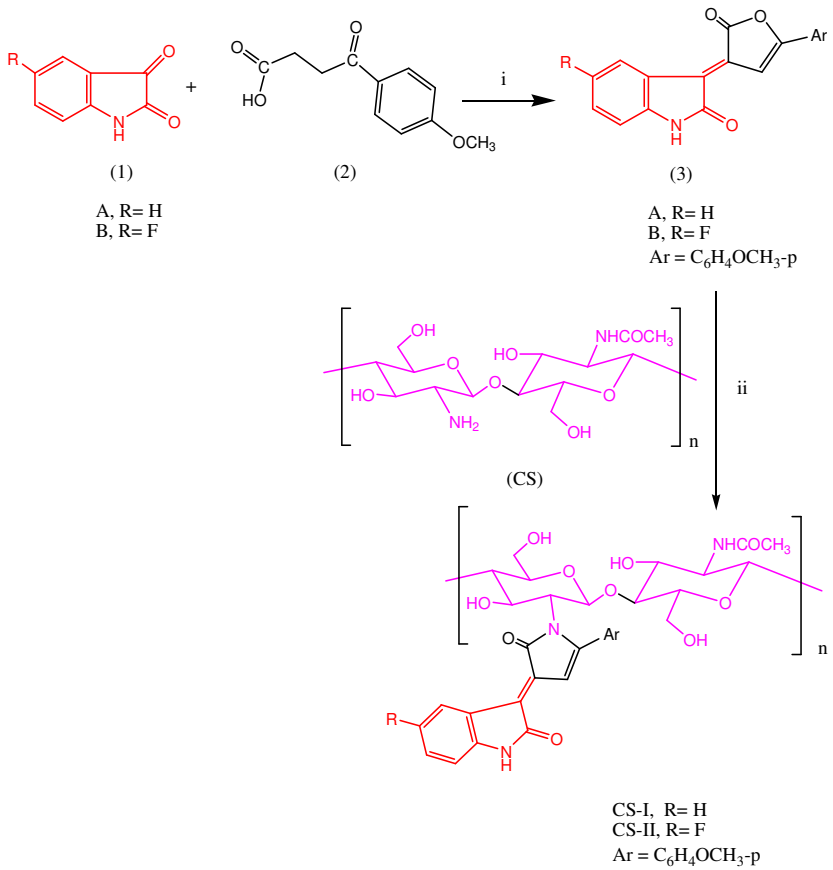


**Scheme1:** Preparation of furanone derivatives and (CS) derivatives i) $Ac_2O$/ Microwave and ii) AcOH/ Microwave

**Table 1**
Elemental analysis, (MW) and (DD %) for CS and (DS) for CS derivatives

| Comp. No. | C% | H% | N% | C/N | MW KDa | DD% | DS |
|---|---|---|---|---|---|---|---|
| Cs | 38.48 | 7.01 | 7.31 | 5.26 | 60 | 93.3 | - |
| Cs-I | 49.61 | 6.35 | 6.41 | 7.74 | - | - | 0.13 |
| CS-II | 47.29 | 6.97 | 5.86 | 8.07 | - | - | 0.15 |

### 3.2.2. FTIR spectroscopy

In the FTIR spectrum of CS as shown in **Fig. 1B** the characteristic peak was a broad band at 3436 $cm^{-1}$ referred to the overlapping of OH and NH ($NH_2$) stretching vibration. Band at 2873 $cm^{-1}$ can be attributed to C-H aliphatic stretching vibration and a peak at 1663 $cm^{-1}$ due to carbonyl group (C=O) of the acetylated unit present in (CS) structure [**7**-**19**].

The interactions between CS and furanone derivatives **3A**or **3B** can be proved by the FTIR spectra for CS-I and CS-II derivatives that represented in **Fig. 1B** and showed shift characteristic peaks compared to (CS) at 3426, 3431 and 2928, 2922$cm^{-1}$ and 1659, 1630 $cm^{-1}$ assigned to (OH, NH($NH_2$), CH aliphatic and (C= O) groups respectively. Additionally, new peaks appeared at 1709 and 1708 $cm^{-1}$ ascribed to (C=O) lactone confirmed the incorporation of furanone moieties in (CS) structure.

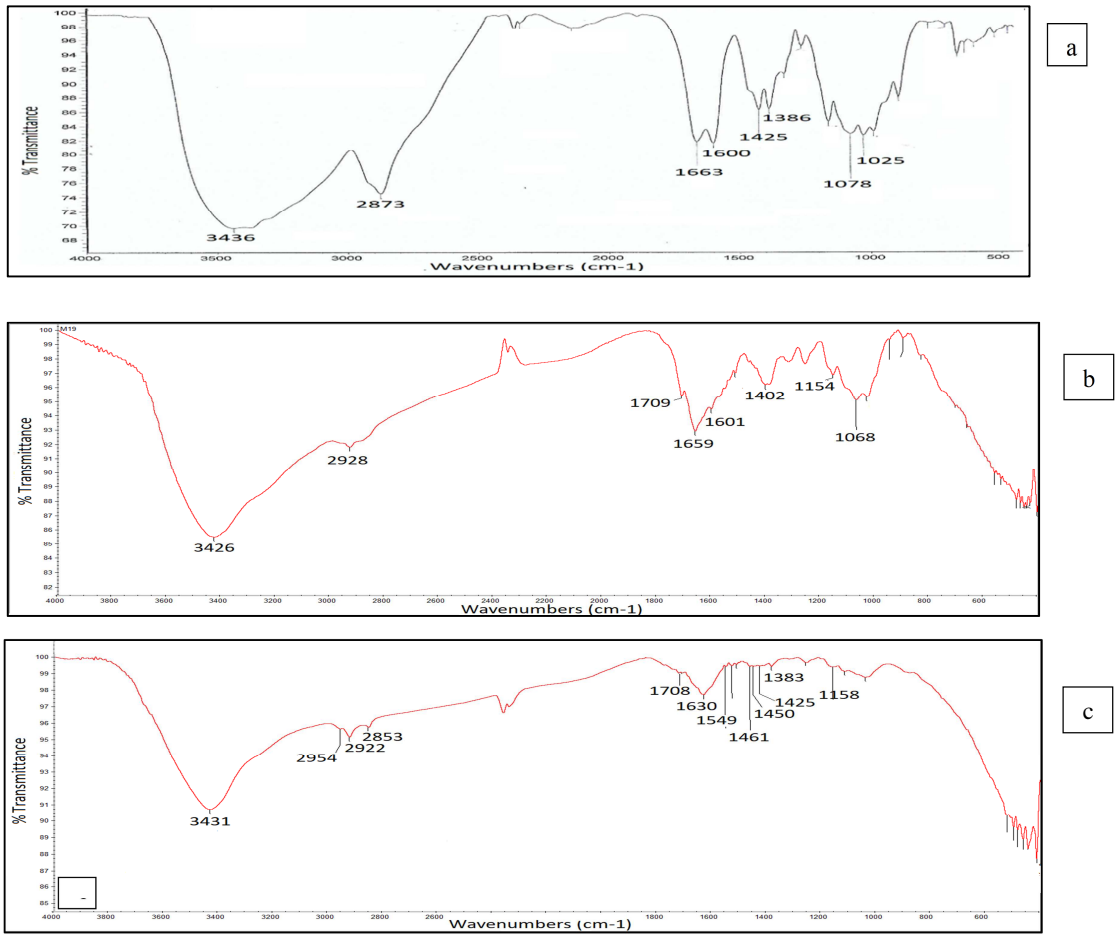


**Fig. 1B**: FTIR of a) CS, b) CS-I and c) CS-II

### 3.2.3. Thermogravimetric Analysis (TGA).

The thermal stability of CS and its derivatives CS-I and CS-II was studied using TGA and represented in (**Fig.2** (**A-C**)). TGA curves showed initial weight losses 12.27%, 13.11% and 46.73% for CS, CS-I and CS-II derivatives respectively at temperature low than 100°C attributed to moisture evaporation due to water molecules bonded with (OH, $NH_2$) groups in CS backbone. The actual degrading step of CS was found at 294.25°C with a mass loss of 40.70% [**7,8,10**]. Furthermore, the onset decomposition temperature for CS-I and CS-II derivatives were 301.78°C and 278.47 °C with weight losses 4.95 % and 19.37% respectively.

TGA analysis referred to slightly higher thermal stability than CS showed by CS-I derivative, while CS-II derivative outlined the lowest thermal stability which pointed to the thermal stability of CS was altered after its reaction with furanones and depended on heterocyclic derivatives [**7-9,10,18**].

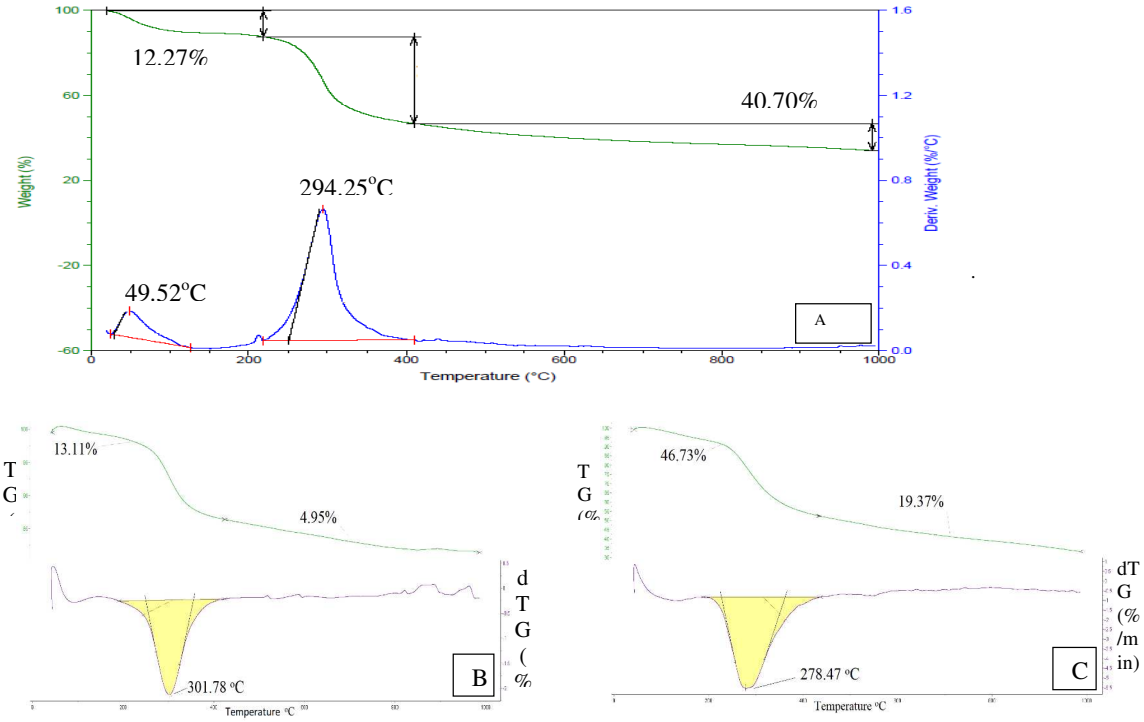


**Fig. 2:** TGA of A) CS, B) CS-I, and CS-II

### 3.2.4. X-Ray Diffraction (XRD)

The crystallinity of CS and modified CS derivatives was studied using XRD patterns which represented in (**Fig. 3**(**A-C**)). The crystallinity nature of CS displayed two peaks at 2Θ =10° (low intensity) and 2Θ =20° (high intensity) [**7-14,18**]. However, XRD patterns for CS derivatives CS-I and CS-II demonstrated its amorphous nature with only one broad peak in the range 2Θ =20-30°, while the peak reported for CS at 2Θ =10° was disappeared may be attributed to incorporate furanone moiety in CS structure which reduced its crystallinity as we reported in previous studies that the crystallinity of CS may be changed after incorporation of different heterocyclic moieties in its backbone [**7,9-12**].

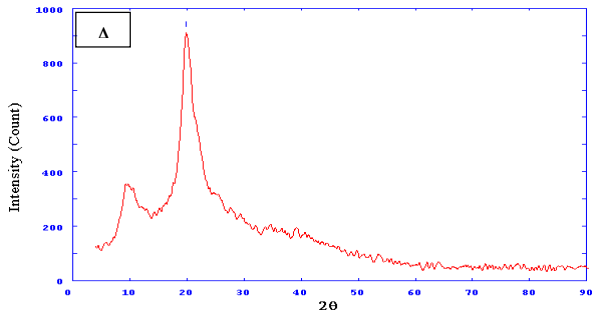

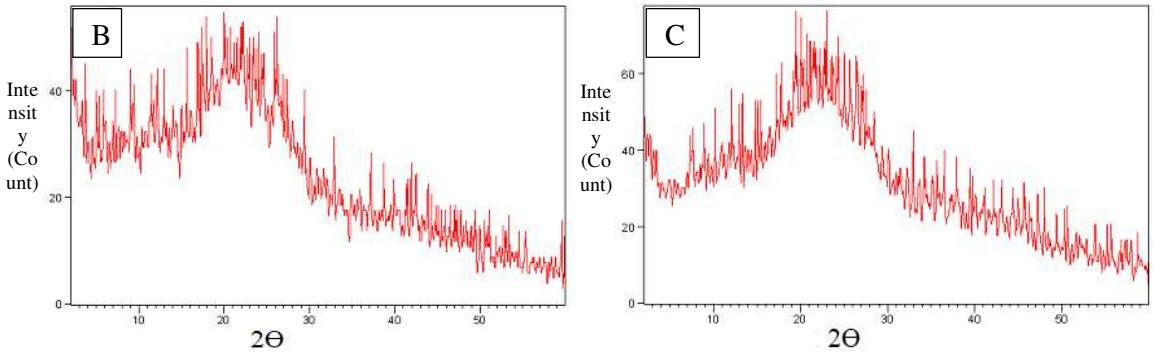


**Fig. 3**: X-Ray of A) CS, B) CS-I, and C) CS-II

### 3.2.5. Scanning Electron Microscopy (SEM)

SEM images were used to characterize the surface morphology of CS and its derivatives at 20 and 50 µm respectively. Chitosan showed the smooth surface as shown in (**Fig. 4A**) [**7-12,14,18**]. Furthermore, the surface morphology of CS-I and CS-II derivatives revealed small deal of crystals adhered on the CS derivatives surfaces as shown in (**Fig. 4(B,C**) respectively confirming that furanone derivatives **3A**or **3B** exhibited capping on the CS surface that agreed with our previous studies which pointed to the CS surface morphology affected after its modification or cross linking with different heterocyclic compounds [**7-12,14,18**].

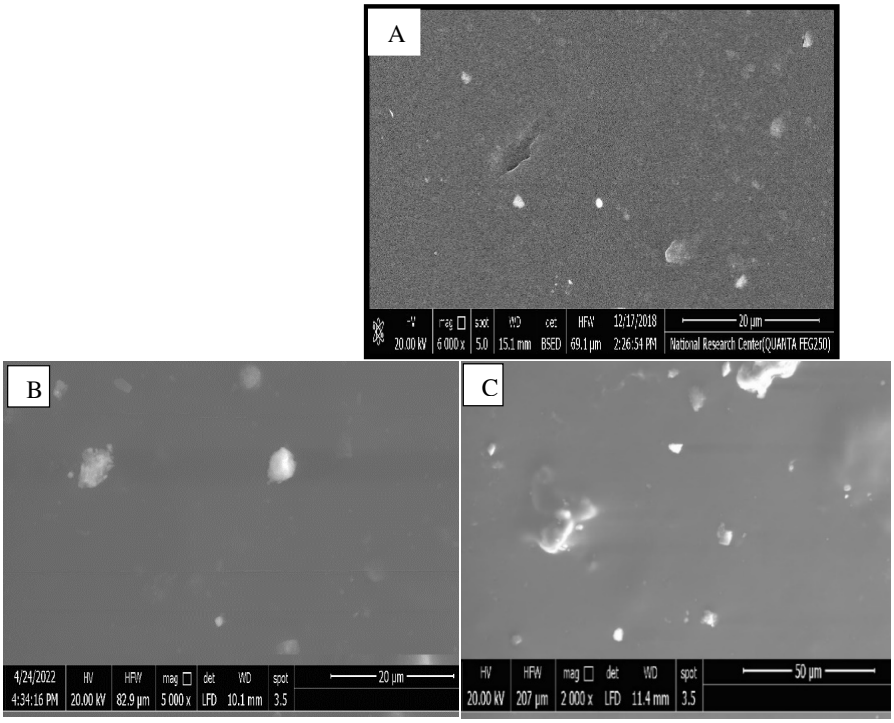


**Fig. 4.** SEM for A) CS, B) CS-I, and C) CS-II

### 3.2.6 Loading Au, Ag or ZnO NPs on CS derivatives CS-I and CS-II

Modified CS nanocomposites derivatives CS-I, II Au, CS-I, II Ag, and CS-I, II ZnO NPs were prepared by the assembling method of dropping Au, Ag or ZnO NPs solutions into soaked CS-I or CSII derivatives in aqueous acetic acid and left under magnetic stirrer overnight then collected using centrifuge. The loading process was confirmed using TEM images for nanocomposites derivatives.

### 3.2.6.1. UV-VIS spectroscopy of Au, Ag and ZnO NPs

UV– visible absorption was used to confirm the formation of gold and silver nanoparticles solution. **Fig. 5** represented UV–vis absorption spectra of prepared Au and Ag NPs and ZnO NPs. The UV–vis absorption of the colloidal suspension showed a strong broad band at 528 and at 418 nm for Au and Ag NPs respectively which related to the surface plasmon resonance (SPR) of gold and silver nanoparticles. However, ZnO NPs revealed a band around 378 nm [**7,17**].

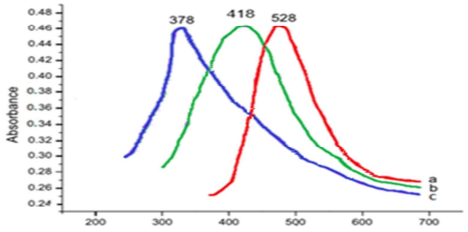


**Fig. 5:** UV-vis spectrum of a) Au NPs, b) Ag NPs and c) ZnO NPs.

### 3.2.6.2. Transmission Electron Microscopy (TEM)

The shapes and particle sizes of Au, Ag, and ZnO nanoparticles and modified CS nanocomposites derivatives CS-I, II Au, CS-I, II Ag, and CS-I, II ZnO NPs were characterized using TEM (**Fig. 6** (**A-J**)). TEM images which measured at 100 nm revealed that Au, Ag and ZnO NPs were predominantly spherical in shape and polydisperse. Moreover, the nanocomposites derivatives displayed a homogeneously distributed, individual nanoparticles, spherical shape and the particle size diameter was found in the range of 9.04 – 41.8 nm which improved successful loading process of CS derivatives on inorganic nanoparticles that agreed with our previous studies which outlined nanocomposites particle size less than 100 nm **[7]**.

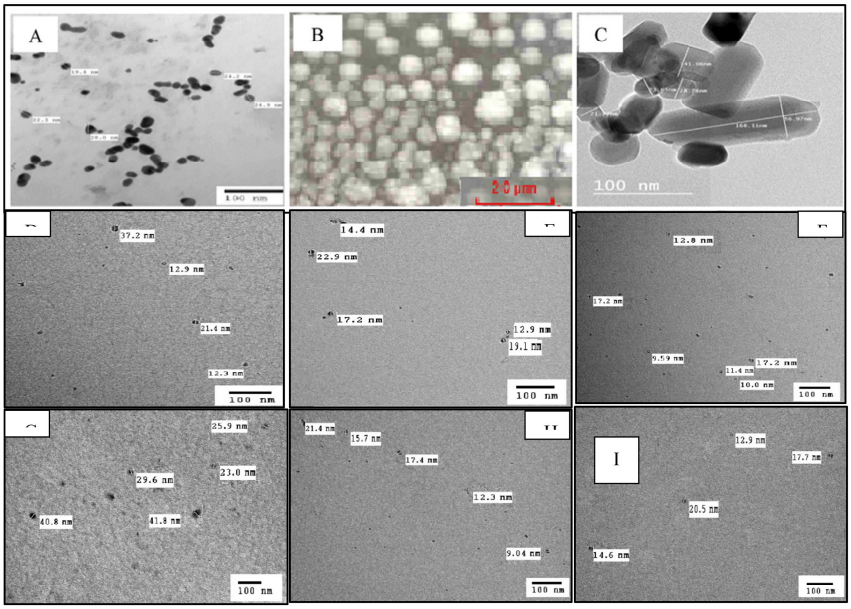


**Fig. 6:** TEM images of (A) Au NPs, (B) Ag NPs, (C) ZnO NPs, (D) CS-I Au NPs, (E) CS-I Ag NP, (F) CS-I ZnO NPs, (G) CS-II Au NPs, (H) CS-II Ag NP and (I) CS-II ZnO NPs

### 3.3. Cytotoxicity Studies

#### 3.3.1. Viability assay

Chemotherapy is one of the most important forms of cancer therapy and it has been a steady growth in the number of available nanoparticles for therapy [**34**]. Chitosan CS is a natural polysaccharide that is widely used as antimicrobial [**7-12**], antioxidant, and anticancer agents due to its essential properties of biodegradability, biocompatibility and non-toxic [**8,35**]. The cytotoxicity of CS, CS-I, CS-II and its nanocomposites against two types of cancer cells **HepG-2** hepatocellular cancer and **MCF-7** breast cancer was evaluated by the viability assay method which tested on a series of concentrations ranging from 31.25 - 500 µg/mL. As represented in (**Fig.7** (**A-F**), there was opposite correlation between samples concentrations and cells viability by increasing sample concentrations cell viability was decreased indicated to increase antitumor activity. Meanwhile, CS, modified CS derivatives and its nanocomposites exhibited antitumor efficiencies toward **HepG-2** and**MCF-7** cells reached to the maximum cell inhibition at concentration 500 µg/mL. At the highest concentration 500 µg/mL, CS-I and CS-II derivatives revealed lower cell viability values 13.69±2.03% ($IC_{50}$ 205.4±8.41 µg/ml) and 10.54±0.92% ($IC_{50}$ 108.84±3.67 µg/ml) respectively compared to CS which displayed cell viability value 25.48±1.66% ($IC_{50}$ 249.17±4.21 µg/ml) against **HepG-2** cancer cell. The same activities appeared toward **MCF-7**cancer cell that showed cell viability values 26.76±1.96% ($IC_{50}$ 280.14±8.72 µg/ml), 16.85±2.13% ($IC_{50}$ 210.75±6.42 µg/ml) and 11.39±0.97% ($IC_{50}$ 151.50±4.98 µg/ml) for CS, CS-I and CS-II, respectively.

The cytotoxicity results for CS-I and CS-II derivatives displayed significantly enhancement might be attributed to the moiety of furanone derivatives **3A**or **3B** incorporated in CS backbone which was reported in our pervious study as key heterocyclic compound used to synthesis new antitumor agents [**27**]. However, significant increases of anticancer activities were obviously for CS-I and CS-II derivatives after loading Ag, Au or ZnO NPs against **HepG-2** and **MCF-7**cells. Especially, ZnO nanocomposites CS-I ZnO NPs and CS-II ZnO NPs derivatives were showed the lowest **HepG-2** cell viability reached to 4.84±0.51% ($IC_{50}$ 61.58±0.98 µg/ml) and 5.28±0.54% ($IC_{50}$ 72.34±2.89 µg/ml) respectively at the concentration 500 µg/mL. Additionally, the inhibitory activity order for the other nanocomposites is CS -I Ag NPs > CS -II Au NPs > CS -II Ag NPs > CS -I Au NPs with cell viability values 6.08±0.44%, 6.75±0.19%, 8.26±0.63% and 8.34±0.62% respectively. Moreover, $IC_{50}$ order is 87.38±2.92< 96.07±3.14% < 116.93±4.01% < 194.79±3.43 µg/ml for CS-I Ag NPs, CS -II Au NPs, CS -I Au NPs and CS -II Ag NPs, respectively. Furthermore, CS-I Ag NPs and CS-I ZnO NPs possessed the minimum cell viability and $IC_{50}$ reached to 5.41±0.63% ($IC_{50}$ 90.34±3.12 µg/ml) and 6.76 ±0.82% ($IC_{50}$ 115.80±3.59 µg/ml) respectively against **MCF-7** cancer cell at the concentration 500 µg/mL. At the same time, the antitumor efficiency for the other nanocomposites displayed in the following order CS-II ZnO NPs >CS-I Au NPs >CS-II Ag NPs > CS-II Au NPs with cell viability reached to 7.46±0.82% ($IC_{50}$ 121.39±3.47 µg/ml), 8.72±0.64% ($IC_{50}$ 124.12±3.65 µg/ml), 9.82±0.64% ($IC_{50}$ 141.84±5.43 µg/ml) and 15.43±2.19% ($IC_{50}$ 180.66±5.529 µg/ml) respectively. From the anticancer evaluation results, it was indicated that the nanocomposites revealed the strongest antitumor activity due to their small particle size and large surface area caused their superior properties in cell permeability, retention and most importantly cellular uptake [**3**]. Mostly metal nanoparticles have always been favored because low cytotoxic activity, their ability to improve the efficacy of anticancer drug and have a tremendous number of applications including cancer treatment [**4**].

## 4. Conclusion

Due to the great biological importance of furanone derivatives, in the present study furanone derivatives based on isatin and/or 5-fluoroisatin derivatives **3A** or **3B** were prepared and used to modify CS to give CS-I and CS-II derivatives via microwave irradiation as a green approach. The new modified chitosan derivatives CS-I and CS-II were characterized by different tools. The highest thermal stability was showed by CS-I derivative also decreasing of crystallinity and irregular surface for CS-Iand CS-II derivatives were observed in XRD and SEM respectively. Nanocomposites were successfully formulated with assembling process of Au, Ag orZnO NPs on CS-I and CS-II and TEM images confirmed the NPs sizes less than 100 nm. Cytotoxicity study results proved that CS-I and CS-II derivatives and its nanocomposites possessed higher antitumor activities potential against **HepG-2**, and **MCF-7** cancer cells compared with CS and could play an important role in biomedical applications.

## 5. Declaration of competing interest

The authors report no conflict of interest. The authors alone are responsible for the content and writing of the article.

## 6. Acknowledgment

We thank Ain Shams University for its financial support with the chemicals used in this research.

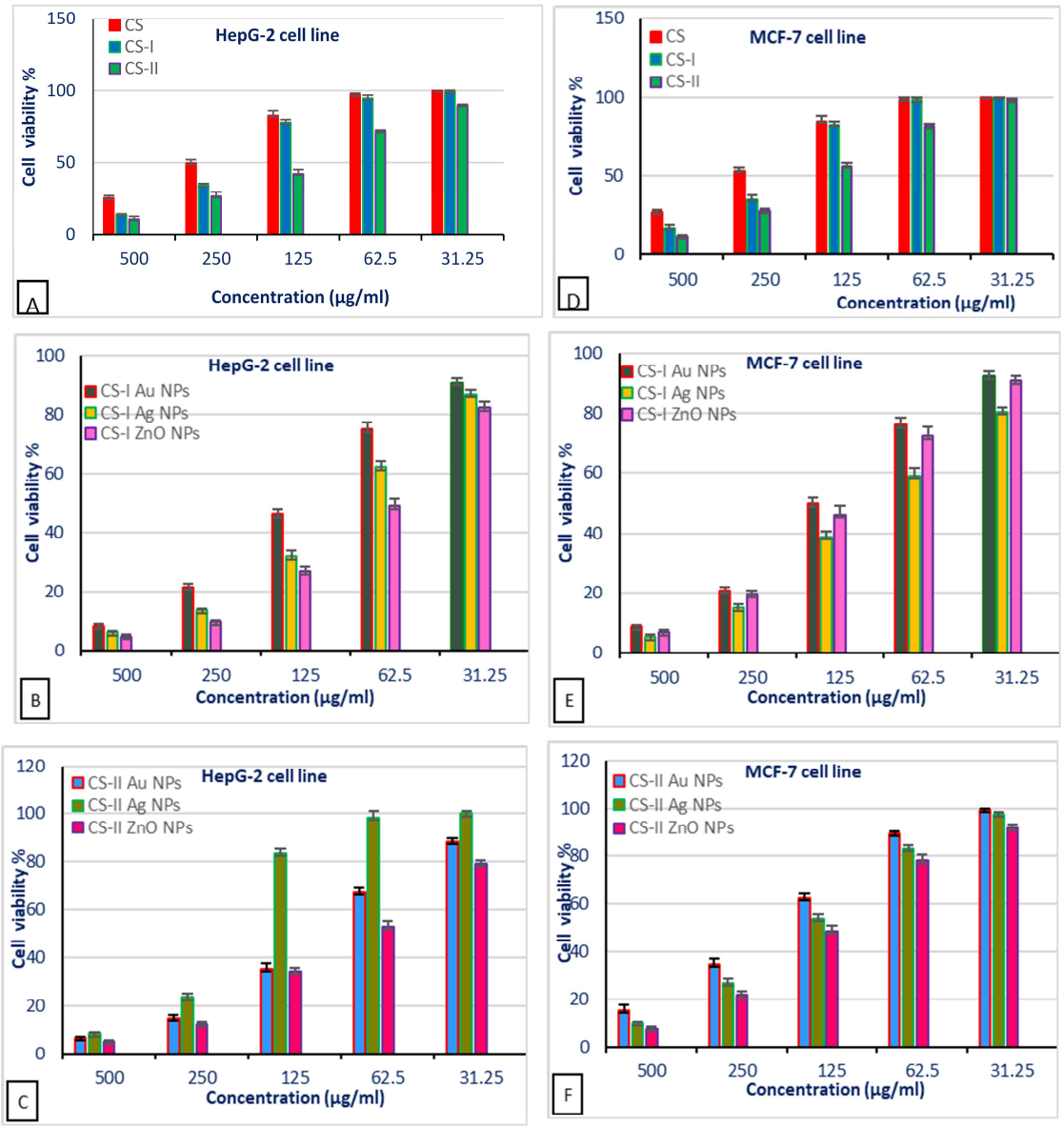


**Fig.7**. Cell viability % toward A,B,C) HepG-2 cell and D,E,F) MCF-7 cell line at concentrations 31.25 - 500 µg/ml respectively for CS, CS-I, CS-II and its nanocomposites.

## 7. Reference

[1] J. Liang, F. Li, Y. Fang, W. Yang, X. An, L. Zhao, Z. Xi, L. Cao, Q. Hu.Cytotoxicity and apoptotic effects of tea polyphenol-loaded chitosan nanoparticles on human hepatoma HepG2 cells, Mater. Sci. Eng. C 36 (2014) 7–13. http://dx.doi.org/10.1016/j.msec.2013.11.039

[2] A. L. Al-Malki, A. Bakkar, E. A. Huwait, E. K. Barbour, K. O. Abulnaja, T. A. Kumosani, S. S. Moselhy, Strigol1/albumin/chitosan nanoparticles decrease cell viability, induce apoptosis and alter metabolomics profile in HepG2 cancer cell line, Biomed. Pharm. 142 (2021) 111960. https://doi.org/10.1016/j.biopha.2021.111960

[3] H. Horo, S. Bhattacharyya, B. Mandal, L. M. Kundu. Synthesis of functionalized silk-coated chitosan-gold nanoparticles and microparticles for target-directed delivery of antitumor agents,

Carbohyd. Polym. 258 (2021) 117659 https://doi.org/10.1016/j.carbpol.2021.117659

[4] K. Priya, M. Vijayakumar, B. Janani. Chitosan-mediated synthesis of biogenic silver nanoparticles (AgNPs), nanoparticle characterisation and in vitro assessment of anticancer activity in human hepatocellular carcinoma HepG2 cells, Int. J. Biol. Macromol. 149 (2020) 844–852. https://doi.org/10.1016/j.ijbiomac.2020.02.007

[5] J. Akinyelu, O. Oladimeji, M. Singh. Lactobionic acid-chitosan functionalised gold-coated poly(lactide-co-glycolide) nanoparticles for hepatocyte targeted gene delivery, Adv. Nat. Sci.: Nanosci. Nanotechnol. 11 (2020) 045017 https://doi.org/10.1088/2043-6254/abc9c3

[6] X. Zhu, L. Shen, Q. Chen, H. Wang, X. Zeng. Anti-hepatoma activity of a new selenium-rich chitosan from 6-Hydroxy esterification of chitosan copper, Mater.Sci. Eng. 782 (2020) 022107 doi:10.1088/1757-899X/782/2/022107

[7] R. A. Elzamly, H. M. Mohamed, M. I. Mohamed, H. T. Zaky, D. R.K. Harding, Nadia G. New sustainable chemically modified chitosan derivatives for different applications: Synthesis and characterization, Arab J. Chem. 14 (2021) 103255. https://doi.org/10.1016/j.arabjc.2021.103255

[8] N. G. Kandile, H. M. Mohamed, New chitosan derivatives inspired onheterocyclic anhydride of potential bioactive for medical applications, Int. J. Biol. Macromol. 182 (2021) 1543–1553. https://doi.org/10.1016/j.ijbiomac.2021.05.076

[9] N. G. Kandile, H. M. Mohamed, Chitosan nanoparticle hydrogel based sebacoyl moiety with remarkable capability for metal ion removal from aqueous systems, Int. J. Biol. Macromol.122 (2019) 578–586. https://doi.org/10.1016/j.ijbiomac.2018.10.198

[10] M. ElS. Ahmed, H. M. Mohamed, M. I. Mohamed, Nadia G. Kandile, Sustainable antimicrobial modified chitosan and its nanoparticles hydrogels: Synthesis and characterization, Int. J. Biol. Macromol.162 (2020) 1388–1397. https://doi.org/10.1016/j.ijbiomac.2020.08.048

[11] N. G. Kandile, M. I. Mohamed, H. T. Zaky, A. S. Nasr, Y. G. Ali, Quinoline anhydride derivatives cross-linked chitosan hydrogels for potential use in biomedical and metal ions adsorption, Polym. Bull. (2021). https://doi.org/10.1007/s00289-021-03633-w

[12] T. H. Abdalla, A. S. Nasr, Gh. Bassioni, D. R. Harding, Nadia G. Kandile, Fabrication of sustainable hydrogels-based chitosan Schiff base and their potential applications, Arab J. Chem. 15 (2022)103511. https://doi.org/10.1016/j.arabjc.2021.103511

[13] I. Kavianinia,P. G. Plieger,N. G. Kandile,D. R. K. Harding, Preparation and characterization of an amphoteric chitosan derivative employing trimellitic anhydride chloride and its potential for colon targeted drug delivery system, Mater. Today Commun. 3 (2015) 78-86. https://doi.org/10.1016/j.mtcomm.2015.03.002

[14] N. G. Kandile, H. M. Mohamed, M. I. Mohamed, New heterocycle modified chitosan adsorbent for metal ions (II) removal from aqueous systems, Int. J. Biol. Macromol. 72 (2015) 110–116. https://doi.org/10.1016/j.ijbiomac.2014.07.042

[15] I. Kavianina, P. G. Plieger, N. J. Cave, G. Gopakumar, M. Dunowasks, N. G Kandile and D. R. K. Harding, Design, and evaluation of a novel chitosan-based system for colon-specific drug delivery, Int. J. Biol. Macromol. 85 (2016)539-546. https://doi.org/10.1016/j.ijbiomac.2016.01.003

[16] H. M. Ibrahim, M. Mostafa, N. G. Kandile, Potential use of N-carboxyethylchitosan in biomedical applications: Preparation, characterization, biological properties, Int. J. Biol. Macromol.149 (2020) 664–671. https://doi.org/10.1016/j.ijbiomac.2020.01.299

[17] N. G. Kandile, H. M. Mohamed, A. S. Nasr, Novel hydrazinocurcumin derivative loaded chitosan, ZnO, and Au nanoparticles formulations for drug release and cell cytotoxicity, Int. J. Biol. Macromol.158 (2020) 1216–1226. https://doi.org/10.1016/j.ijbiomac.2020.05.015

[18]N. G. Kandile, M. I. Mohamed, H. T. Zaky, A. S. Nasr, E. Abdel-Bary, Synthesis and properties of chitosan hydrogels modified with heterocycles. Carbohydr. polym. 75 (4) (2009) 580-585. https://doi.org/10.1016/j.carbpol.2008.08.024

[19] I. Kavianinia, P.G. Plieger, N.G. Kandile, D.R.K. Harding, In vitro evaluation of spraydried chitosan microspheres crosslinked with pyromellitic dianhydride for oral colon-specific delivery of protein drugs, J. Appl. Polym. Sci. 40514 (2014) 1-7. https://www.researchgate.net/publication/260412803

[20] A. B. Seabra, G. K. Fabbri, M. T. Pelegrino, L. C. Silva, T. Rodrigues.Synthesis, characterization and cytotoxicity of S-nitrosomercaptosuccinicacid-containing alginate/chitosan nanoparticles, J. Phys.: Conf.

Series 838 (2017) 012032. doi :10.1088/1742-6596/838/1/012032

[21] M. M. Metwally, R. Mu. ntilde;oz-Espi, I. Youssef, D. S. Badawy, M., Synthesis of 3-dimensional chitosan/carboxymethyl cellulose/ZnO biopolymer hybrids by ionotropic gelation for application in drug delivery, EJCEH. 65 (1) (2022) 299-307.doi: 10.21608/EJCHEM.2021.76761.3765

[22] R. Abdel-Monem, S. T. Gaballah, H. El-Nazer, S. Rabie, In vitro antibacterial activity of maleamates functionalized-chitosan-PVC/silver nanocomposites, EJCEH. 63(4) (2020) 1305-1323. 10.21608/EJCHEM.2019.14908.1904

[23] A. M. Omer, Y. A. Ammar, G. A. Mohamed, Y. S. Abd elbaky, T. M. Tamer, Preparation of isatin/chitosan schiff Base as novel antibacterial biomaterials, EJCEH 62 Special Issue (Part 1) Innovation in Chemistry(2019) 123-131. 10.21608/EJCHEM.2019.7766.1614

[24] S. A.-S. Khalil, O. Ghazy, A. Elnaggar, S. Mahdy, M. Senna,Polymerization of acrylic acid on chitosan by gamma radiation and its application for the removal of metal ions from aqueous solutions EJCEH. 65(1) (2022) 279-286.DOI:10.21608/EJCHEM.2021.74367.3672

[25] M. M. Sabet, T. M. Tamer, A. M. Omer, W. M. Salem, M. A. Hassan, M. H. Gouda, M. Mohyeldin, Effect of tween 20 as plasticizer on cinnamyl chitosan membranes: Preparation, characterization and antimicrobial evaluation, EJCEH. 63(6) (2020) 1989-1998. DOI:10.21608/EJCHEM.2019.6679.1561

[26] S. A. Loutfy, H. M. Alam El-Din, M. H. Elberry, N. G. Allam, M. T. M. Hasanin, A. M. Abdellah. Synthesis, characterization and cytotoxic evaluation of chitosan nanoparticles: in vitro liver cancer model, Adv. Nat. Sci.: Nanosci. Nanotechnol. 7 (2016) 035008.DOI:10.1088/2043-6262/7/3/035008

[27] H. T. Zaky, M. I. Mohamed, N. G. Kandile. Efficient synthesis of new oxindol-based heterocyclic entities via indolin-2-one derivatives, Arab J. Chem. 7 (2014) 630–638. http://dx.doi.org/10.1016/j.arabjc.2014.01.005

[28] P. G. Gan, S. T. Sam, M. F. Abdullah, M. F. Omar, W. K. Tan, Water resistance and biodegradation properties of conventionally-heated and microwave-cured cross-linked cellulose nanocrystal/chitosan composite films, PolymDegrad Stab 188 (2021) 109563.www.elsevier.com/locate/polymdegradstab

[29] G. Priyadarshi, N. P. Raval, M. H. Trivedi, Microwave-assisted synthesis of cross-linked chitosan-metal oxide nanocomposite for methyl orange dye removal from unary and complex effluent matrices, Int. J. Biol. Macromol. 219 (2022) 53-67. https://doi.org/10.1016/j.ijbiomac.2022.07.239

[30] T. Mosmann, Rapid colorimetric assay for cellular growth and survival application to proliferation and cytotoxicity assays, J. Immunol. Method. 65 (1983) 55-63.https://doi.org/10.1016/0022-1759(83)90303-4Get rights and content

[31] S. M. Gomha, S. M. Riyadh, E. A. Mahmmoud, M. M. Elaasser, Synthesis and anticancer activities of thiazoles, 1,3-thiazines, and thiazolidine using chitosan-grafted-poly(vinylpyridine) as basic catalyst, Heterocycles 91(6) (2015) 1227-1243.DOI:10.3987/COM-15-13210

[32] T. Aziz, F. Rahim, R. Ullah, A. Ullah, F. Haq, F. U. Khan, M. Kiran, N. S. Khattak, M. Iqbal. Synthesis and biological evaluation of Isatin based Thiazole derivatives, Biomed. J. Sci. Res.28 (5) (2020) 21919-21925. DOI: 10.26717/BJSTR.2020.28.004704

[33] M. Kasaai, J. Arul, G. Charlet, Intrinsic viscosity–molecular weight relationship for chitosan, J. Polym. Sci. B Polym. Phys. 38 (2000) 2591–2598.https://doi.org/10.1002/1099-0488(20001001)38:19<2591::AID-POLB110>3.0.CO;2-6

[34] L. Li, P. Zhang, C. Li, Y. Guo, K. Sun. In vitro/vivo antitumor study of modified-chitosan/carboxymethyl chitosan “boosted” charge-reversal nanoformulation, CarbohydrPolym 269 (2021) 118268 https://doi.org/10.1016/j.carbpol.2021.118268

[35] Y. Mi, Y. Chen, G. Gu, Q. Miao, W. Tan, Q. Li, Z. Guo. New synthetic adriamycin-incorporated chitosan nanoparticles with enhanced antioxidant, antitumor activities and pH-sensitive drug release, Carbohydr. Polym. 273 (2021) 118623 https://doi.org/10.1016/j.carbpol.2021.118623